

# Spatial state Stokes-operator squeezing and entanglement for optical beams

M. T. L. Hsu,<sup>1,2</sup> W. P. Bowen,<sup>3</sup> and P. K. Lam<sup>1</sup>

<sup>1</sup>*ARC COE for Quantum-Atom Optics, Australian National University, Canberra, ACT 0200, Australia.*

<sup>2</sup>*Present address: Department of Chemistry, Stanford University, Palo Alto, CA 94305, U.S.A.*

<sup>3</sup>*School of Physical Sciences, University of Queensland, Brisbane, QLD 4072, Australia.*

(Dated: September 4, 2021)

The transverse spatial attributes of an optical beam can be decomposed into the position, momentum and orbital angular momentum observables. The position and momentum of a beam is directly related to the quadrature amplitudes, whilst the orbital angular momentum is related to the polarization and spin variables. In this paper, we study the quantum properties of these spatial variables, using a representation in the Stokes-operator basis. We propose a spatial detection scheme to measure all three spatial variables and consequently, propose a scheme for the generation of spatial Stokes operator squeezing and entanglement.

PACS numbers: 42.50, 42.30

## I. INTRODUCTION

Squeezed and entangled bright optical fields are essential resources in the continuous variable quantum optics and quantum information communities [1]. To date, the vast majority of research has been focused on fields which exhibit non-classical features on their amplitude and phase quadratures. Recently, however, a number of papers have been published on squeezing and entanglement of other field variables, and in particular the polarization [2] and spatial structure [3, 4, 5, 6]. These variables can be directly related to momentum components of the field. The quadrature amplitudes are associated with the *transverse linear momentum* of the field, whilst the polarization states and spatial states considered to date are respectively associated to the *spin angular momentum* and the *transverse angular momentum*. We immediately see why interaction of a polarization squeezed field with an atomic ensemble can yield atomic spin squeezing [7], and why spatially entangled light can be used to test the EPR paradox with position and momentum variables [5] as was originally proposed by Einstein, Podolsky and Rosen [8].

The correspondence of non-classical polarization and spatial states with non-classical momentum states immediately raises the question of whether non-classical *orbital angular momentum* states can also be generated. Such states have been under investigation for some time in the discrete variable regime. Techniques have been established to detect the orbital angular momentum properties of single photons [9, 10, 11]; and discrete-variable multi-dimensional entanglement between orbital angular momentum states has been proposed [12, 13] and demonstrated [14]. However, to date, non-classical orbital angular momentum states have not been investigated for the continuous variable regime, that is relevant in many applications [15, 16, 17, 18, 19, 20, 21]. We investigate these continuous variable orbital angular momentum quantum states, proposing techniques for both generation and detection. Many applications have been proposed for optical orbital angular momentum in the classical domain,

ranging from the generation of counter-rotating superpositions in Bose-Einstein condensates [22, 23], and transfer of orbital angular momentum from an atomic ensemble to a light field [24], to optical angular momentum transfer to trapped particles [25, 26, 27]. It should be noted that light with orbital angular momentum has also been applied to achieve super-resolution imaging of molecules and proteins in biological systems, via techniques such as *stimulated emission depletion* (STED) [28]. Non-classical orbital angular momentum states offer the prospect to improve these processes, and to generate non-classical orbital angular momentum states in macroscopic physical systems.

Ref. [5] proposed EPR entanglement of the position-momentum observables of optical fields, and this has recently been experimentally observed [6]. In these references, entanglement was present only for one transverse axis of the beam, and analysis only required consideration of the TEM<sub>00</sub> and TEM<sub>01</sub> modes. One of the strengths of entanglement in the spatial domain is access to higher dimensional spaces. Here we extend the work of Refs. [5, 6] to include both transverse beam axes, in a formalism easily extended to higher order TEM modes. In the process, orbital angular momentum is introduced as an entanglement variable in addition to beam position and momentum. These quantum variables can be represented on a spatial version of the Poincaré sphere commonly used for analysis of polarization quantum states. We propose a scheme to measure their signal and noise properties, via a spatial Stokes detection scheme; and finally introduce a scheme to generate spatial Stokes-operator squeezing and entanglement.

## II. SPATIAL STOKES OPERATORS

Spatial quantum states exist in an infinite dimensional Hilbert space, which may be conveniently expanded in a basis of TEM<sub>pq</sub> modes. After such an expansion the positive frequency part of the electric field operator,  $\hat{\mathcal{E}}^+(\mathbf{r})$ , can be written explicitly in terms of the double-subscript

sum

$$\hat{\mathcal{E}}^+(\mathbf{r}) = i\sqrt{\frac{\hbar\omega}{2\epsilon_0 V}} \sum_{p,q=0}^{\infty} \hat{a}_{pq} u_{pq}(\mathbf{r}) \quad (1)$$

where  $\hat{a}_{pq}$  and  $u_{pq}(\mathbf{r})$  are the photon annihilation operator and the normalized transverse beam amplitude function, respectively, associated with the  $\text{TEM}_{pq}$  mode. The photon annihilation operator  $\hat{a}_{pq}$  can be formally defined with the projection of the transverse beam amplitude function with the positive frequency part of the electric field operator, given by

$$\hat{a}_{pq} = \iint_{-\infty}^{\infty} dx dy \hat{\mathcal{E}}^+(x, y) u_{pq}(x, y). \quad (2)$$

Within this basis, it is natural to consider pairs of modes with amplitude function that correspond to a physical  $\pi/2$  rotation in the transverse plane. That is, modes of the form  $\text{TEM}_{pq}$  and  $\text{TEM}_{qp}$ , with  $p$  and  $q$  interchanged ( $p \neq q$ ). Pairs of this form are naturally described by a set of spatial Stokes operators  $\hat{S}_i^{(p,q)}$  where  $i \in \{0, 1, 2, 3\}$ , that can be represented by a Poincaré sphere [29] in direct analogy to polarization Stokes operators [30], as shown in Fig. 1.

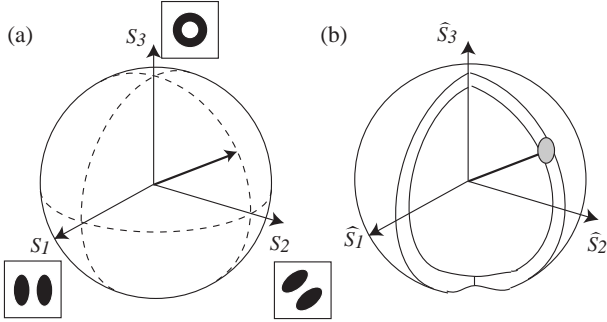


FIG. 1: (a) Poincaré sphere representation based on the spatial modes  $\text{TEM}_{10}$  and  $\text{TEM}_{01}$ .  $S_1$  is the Stokes variable for the  $u_{01}(\mathbf{r})$  and  $u_{10}(\mathbf{r})$  modes,  $S_2$  is the Stokes variable for the  $u_{01}^{45^\circ}(\mathbf{r})$  and  $u_{10}^{45^\circ}(\mathbf{r})$  modes, and  $S_3$  is the Stokes variable for the  $u_{01}^{+1}(\mathbf{r})$  and  $u_{01}^{-1}(\mathbf{r})$  modes. (b) Poincaré sphere representation for the spatial Stokes operators. The shaded area indicates the quantum noise associated with the mean amplitude of the Stokes operator.

Using the definition of the classical Stokes parameters [29], corresponding quantum mechanical spatial Stokes operators are defined as

$$\begin{aligned} \hat{S}_0 &= \hat{a}_{pq}^\dagger \hat{a}_{pq} + \hat{a}_{qp}^\dagger \hat{a}_{qp} \\ \hat{S}_1 &= \hat{a}_{pq}^\dagger \hat{a}_{pq} - \hat{a}_{qp}^\dagger \hat{a}_{qp} \\ \hat{S}_2 &= \hat{a}_{pq}^\dagger \hat{a}_{qp} e^{i\theta} + \hat{a}_{qp}^\dagger \hat{a}_{pq} e^{-i\theta} \\ \hat{S}_3 &= i\hat{a}_{qp}^\dagger \hat{a}_{pq} e^{-i\theta} - i\hat{a}_{pq}^\dagger \hat{a}_{qp} e^{i\theta} \end{aligned} \quad (3)$$

where  $\theta$  is the phase difference between the  $\text{TEM}_{pq}$  and  $\text{TEM}_{qp}$  modes. As is the case with polarization, the spatial Stokes operators obey commutation relations. By using the commutation relations of the photon annihilation and creation operators,  $[\hat{a}_{mn}, \hat{a}_{jk}] = \delta_{mj} \delta_{nk}$ , the Stokes-operator commutation relations can be found to be

$$[\hat{S}_i, \hat{S}_j] = 2i\epsilon_{ijk} \hat{S}_k \quad (4)$$

where  $\epsilon_{ijk}$  is the Levi-Civita tensor.

Each Stokes operator characterizes a different spatial property of the field.  $\hat{S}_0$  represents the beam intensity, whilst the Stokes vector  $(\hat{S}_1, \hat{S}_2, \hat{S}_3)$  characterizes its transverse momentum.  $\hat{S}_1$  and  $\hat{S}_2$  respectively quantify the relative proportions of horizontal to vertical transverse momentum, and  $45^\circ$  to  $-45^\circ$  diagonal transverse momentum; whilst  $\hat{S}_3$  weights left to right orbital angular momentum.

The spatial Poincaré sphere can be fully spanned by spatially overlapping two orthogonal  $\text{TEM}_{pq}$  and  $\text{TEM}_{qp}$  modes. The diagonal modes, for example, are given by  $u_{pq}^{45^\circ}(\mathbf{r}) = u_{qp}(\mathbf{r}) - u_{pq}(\mathbf{r})$  and  $u_{qp}^{45^\circ}(\mathbf{r}) = u_{qp}(\mathbf{r}) + u_{pq}(\mathbf{r})$ , and respectively yield Stokes vectors oriented along the negative and positive  $\hat{S}_2$  axis of the Poincaré sphere. The Laguerre-Gauss modes  $\text{LG}_{0q}$  with orbital angular momentum  $q$  and  $-q$ , are given by  $u_{0q}^{+l}(\mathbf{r}) = u_{0q}(\mathbf{r}) + iu_{q0}(\mathbf{r})$  and  $u_{0q}^{-l}(\mathbf{r}) = u_{0q}(\mathbf{r}) - iu_{q0}(\mathbf{r})$ , yielding Stokes vectors oriented along the  $\hat{S}_3$  axis. For example, the intensity distributions for the diagonal and Laguerre-Gauss modes, generated from the combinations of  $\text{TEM}_{10}$  and  $\text{TEM}_{01}$  modes, are shown in Fig. 2.

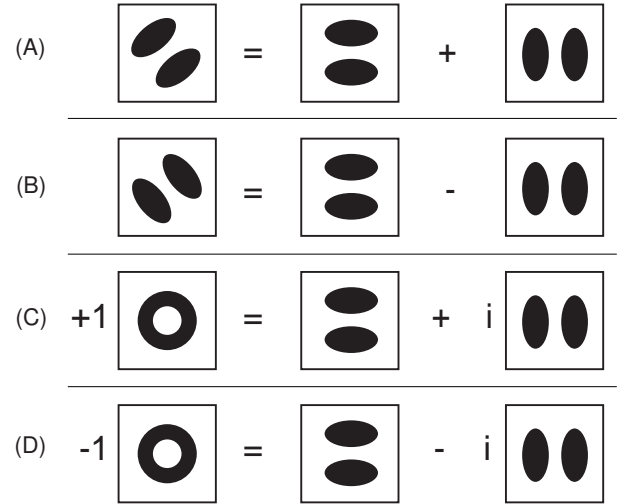


FIG. 2: Intensity distribution for the modes given by (A)  $u_{01}^{45^\circ}(\mathbf{r}) = u_{01}(\mathbf{r}) + u_{10}(\mathbf{r})$ , (B)  $u_{10}^{45^\circ}(\mathbf{r}) = u_{01}(\mathbf{r}) - u_{10}(\mathbf{r})$ , (C)  $u_{01}^{+1}(\mathbf{r}) = u_{01}(\mathbf{r}) + iu_{10}(\mathbf{r})$ , and (D)  $u_{01}^{-1}(\mathbf{r}) = u_{01}(\mathbf{r}) - iu_{10}(\mathbf{r})$ .

Since the diagonal and orbital modes can be generated purely from two orthogonal  $\text{TEM}_{pq}$  and  $\text{TEM}_{qp}$  modes,

only by changing the phase between the modes, these sets of modes obey the  $SU(2)$  group properties. At this point, we restrict our analysis to the  $TEM_{10}$  and  $TEM_{01}$  modes, for illustrative purposes. In principle, our analysis is valid for all orthogonal  $TEM_{pq}$  and  $TEM_{qp}$  modes.

### III. SPATIAL STOKES DETECTION

Now that the spatial Stokes operators have been defined, we consider a system for their detection. Analogous to polarization Stokes operator detection, the spatial Stokes detection requires two separate photodiodes, a modal phase shifter, and a mode separator.

A modal phase shifter is a device that introduces a relative phase shift between the two orthogonal  $TEM_{10}$  and  $TEM_{01}$  modes. The modal phase shifter can be constructed using a pair of cylindrical lenses with variable lens separation, as shown in Fig. 3 (f). The pairing of cylindrical lenses introduces an astigmatic Gouy phase shift between the  $TEM_{10}$  and  $TEM_{01}$  modes. In order to introduce  $\pi$  and  $\pi/2$  modal phase shift, the lens separation is given by  $2f$  and  $\sqrt{2}f$ , respectively, where  $f$  is the focal length of the cylindrical lens. Ref. [21] contains a detailed analysis of the  $\pi$  and  $\pi/2$  modal phase shifters.

A mode separator (MS) is a device that separates the two orthogonal  $TEM_{10}$  and  $TEM_{01}$  modes and can be constructed using an asymmetric Mach-Zehnder interferometer [31], as shown in Fig. 3 (e). Due to the odd and even numbers of reflections in each interferometer arm, different interference conditions for the  $TEM_{01}$  and  $TEM_{10}$  modes are present. The resulting outputs from the interferometer is a separation of even and odd (defined along one spatial axis) spatial modes [31].

Measurements of the total signal and noise, which correspond to a measurement of  $\hat{S}_0$ , are given by the sum of the photocurrents as shown in Fig. 3 (a). Measurement of  $\hat{S}_1$  involves taking the subtraction between the photocurrent outputs corresponding to mode components  $TEM_{10}$  and  $TEM_{01}$ , as shown in Fig. 3 (b). Measurement of  $\hat{S}_2$  involves subtraction of the diagonal mode components and is obtained by phase shifting one mode by  $\pi$  with respect to the other and then taking the subtraction of the photocurrent signals, given in Fig. 3 (c).  $\hat{S}_3$  is measured by decomposing the Laguerre-Gauss mode into its  $TEM_{10}$  and  $TEM_{01}$  modes using  $\pi$  and  $\pi/2$  modal phase shifters, as shown in Fig. 3 (d).

The photon annihilation operators in Eq. (3) can be written in the form  $\hat{a}_{pq} = \alpha_{pq} + \delta\hat{a}_{pq}$ , where  $\alpha_{pq}$  describes the mean amplitude part and  $\delta\hat{a}_{pq}$  is the quantum noise operator. Using the linearized formalism, where second order terms in the fluctuation operator are neglected (i.e.  $|\alpha_{pq}|^2 \gg |\langle \delta\hat{a}_{pq}^2 \rangle|$ ), the mean amplitudes of the Stokes operators in Eq. (3), in terms of the  $TEM_{10}$  and  $TEM_{01}$

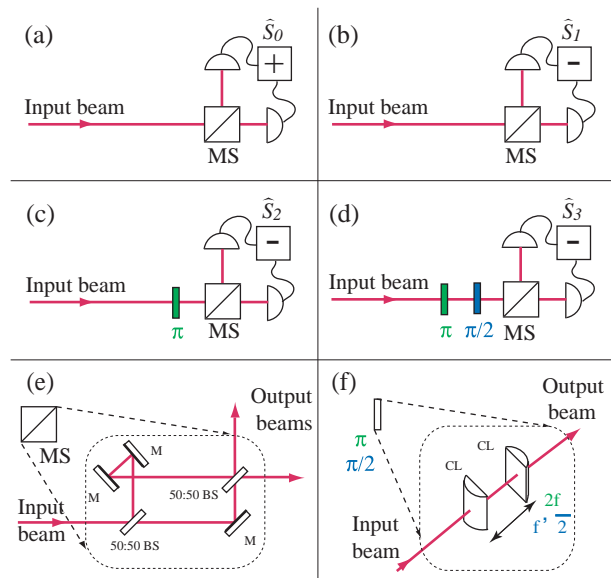


FIG. 3: Measurements of (a)  $\hat{S}_0$ , (b)  $\hat{S}_1$ , (c)  $\hat{S}_2$  and (d)  $\hat{S}_3$ . (e) An example of a mode separator (MS) is an asymmetric Mach-Zehnder interferometer. (f) The  $\pi$  and  $\pi/2$  modal phase shifters could be constructed using a pair of cylindrical lenses with lens separation given by  $2f$  and  $\sqrt{2}f$ , respectively.  $f$  is the focal length of the cylindrical lenses, M is a mirror, 50:50 BS is a symmetric non-polarizing beam-splitter.

modes, are therefore given by

$$\begin{aligned}
 \langle \hat{S}_0 \rangle &= \alpha_{10}^2 + \alpha_{01}^2 = N \\
 \langle \hat{S}_1 \rangle &= \alpha_{10}^2 - \alpha_{01}^2 \\
 \langle \hat{S}_2 \rangle &= 2\alpha_{10}\alpha_{01} \cos \theta \\
 \langle \hat{S}_3 \rangle &= 2\alpha_{10}\alpha_{01} \sin \theta
 \end{aligned} \tag{5}$$

where  $\alpha_{01}$  and  $\alpha_{10}$  are the mean amplitude terms corresponding to modes  $u_{01}(\mathbf{r})$  and  $u_{10}(\mathbf{r})$ , respectively.  $\langle \hat{S}_0 \rangle = N$  is the total mean number of photons,  $\langle \hat{S}_1 \rangle$  is the difference in the mean number of photons in the  $u_{10}(\mathbf{r})$  and  $u_{01}(\mathbf{r})$  modes,  $\langle \hat{S}_2 \rangle$  is the difference in the mean number of photons in the  $u_{01}^{45^\circ}(\mathbf{r})$  and  $u_{10}^{45^\circ}(\mathbf{r})$  modes and  $\langle \hat{S}_3 \rangle$  is the difference in the mean number of photons in the  $u_{01}^{+1}(\mathbf{r})$  and  $u_{01}^{-1}(\mathbf{r})$  modes.

The Stokes operators of Eq. (3) can be expanded in terms of quadrature operators with the general form  $\hat{X}_{\alpha_{pq}}^\phi = e^{-i\phi} \delta\hat{a}_{pq} + e^{i\phi} \delta\hat{a}_{pq}^\dagger$ , and their variances are then

given in general by

$$\begin{aligned}
\langle(\delta\hat{S}_0)^2\rangle &= \alpha_{10}^2\langle(\delta\hat{X}_{a_{10}}^+)^2\rangle + \alpha_{01}^2\langle(\delta\hat{X}_{a_{01}}^+)^2\rangle \\
&\quad + 2\alpha_{10}\alpha_{01}\langle\delta\hat{X}_{a_{10}}^+\delta\hat{X}_{a_{01}}^+\rangle \\
\langle(\delta\hat{S}_1)^2\rangle &= \alpha_{10}^2\langle(\delta\hat{X}_{a_{10}}^+)^2\rangle + \alpha_{01}^2\langle(\delta\hat{X}_{a_{01}}^+)^2\rangle \\
&\quad - 2\alpha_{10}\alpha_{01}\langle\delta\hat{X}_{a_{10}}^+\delta\hat{X}_{a_{01}}^+\rangle \\
\langle(\delta\hat{S}_2)^2\rangle &= \alpha_{10}^2\langle(\delta\hat{X}_{a_{10}}^{-\theta})^2\rangle + \alpha_{01}^2\langle(\delta\hat{X}_{a_{01}}^\theta)^2\rangle \\
&\quad + 2\alpha_{10}\alpha_{01}\langle\delta\hat{X}_{a_{10}}^{-\theta}\delta\hat{X}_{a_{01}}^\theta\rangle \\
\langle(\delta\hat{S}_3)^2\rangle &= \alpha_{10}^2\langle(\delta\hat{X}_{a_{10}}^{-\theta+\frac{\pi}{2}})^2\rangle + \alpha_{01}^2\langle(\delta\hat{X}_{a_{01}}^{\theta-\frac{\pi}{2}})^2\rangle \\
&\quad + 2\alpha_{10}\alpha_{01}\langle\delta\hat{X}_{a_{10}}^{-\theta+\frac{\pi}{2}}\delta\hat{X}_{a_{01}}^{\theta-\frac{\pi}{2}}\rangle
\end{aligned} \tag{6}$$

where  $\hat{X}_{a_{pq}}^+ = \hat{X}_{a_{pq}}^{\phi=0}$  and  $\hat{X}_{a_{pq}}^- = \hat{X}_{a_{pq}}^{\phi=\pi/2}$  are respectively the amplitude and phase quadrature operators of the  $\text{TEM}_{pq}$  mode.

Non-classical optical orbital angular momentum states can be constructed by spatially overlapping a set of orthogonal non-classical  $\text{TEM}_{pq}$  fields, in analogy to the work of Refs. [5, 6] for transverse spatial entanglement. In such a scenario, no correlations should exist between the quadratures of the different input fields, such that  $\langle\delta\hat{X}_{a_{10}}^{\phi_1}\delta\hat{X}_{a_{01}}^{\phi_2}\rangle = 0, \forall\{\phi_1, \phi_2\}$ . Making this assumption, which we will adopt henceforth, the variances of the Stokes operators are simplified to

$$\begin{aligned}
\langle(\delta\hat{S}_0)^2\rangle &= \alpha_{10}^2\langle(\delta\hat{X}_{a_{10}}^+)^2\rangle + \alpha_{01}^2\langle(\delta\hat{X}_{a_{01}}^+)^2\rangle \\
\langle(\delta\hat{S}_1)^2\rangle &= \alpha_{10}^2\langle(\delta\hat{X}_{a_{10}}^+)^2\rangle + \alpha_{01}^2\langle(\delta\hat{X}_{a_{01}}^+)^2\rangle \\
\langle(\delta\hat{S}_2)^2\rangle &= \alpha_{10}^2\langle(\delta\hat{X}_{a_{10}}^{-\theta})^2\rangle + \alpha_{01}^2\langle(\delta\hat{X}_{a_{01}}^\theta)^2\rangle \\
\langle(\delta\hat{S}_3)^2\rangle &= \alpha_{10}^2\langle(\delta\hat{X}_{a_{10}}^{-\theta+\frac{\pi}{2}})^2\rangle + \alpha_{01}^2\langle(\delta\hat{X}_{a_{01}}^{\theta-\frac{\pi}{2}})^2\rangle.
\end{aligned} \tag{7}$$

#### IV. SPATIAL STOKES SQUEEZING

An examination of Eq. (7) shows that simultaneous squeezing of at least two spatial Stokes operators is possible, using two quadrature squeezed input fields. Hence, a spatial Stokes squeezed state can be used to enhance relative measurements of momentum variables along multiple axes. This is best illustrated by considering a few examples.

Simultaneous squeezing of  $\hat{S}_0$ ,  $\hat{S}_1$  and  $\hat{S}_2$  can be achieved through the in-phase ( $\theta = 0$ ) spatial overlap of amplitude squeezed  $\text{TEM}_{10}$  and  $\text{TEM}_{01}$  modes (i.e.  $\langle(\delta\hat{X}_{a_{10}}^+)^2\rangle < 1$  and  $\langle(\delta\hat{X}_{a_{01}}^+)^2\rangle < 1$ ). This spatial squeezed state could be combined with a bright  $\text{TEM}_{00}$  beam to allow enhanced measurements of the transverse momentum of the  $\text{TEM}_{00}$  beam along any axis on the Poincaré sphere within the plane formed by  $\hat{S}_1$  and  $\hat{S}_2$ . Simultaneous squeezing is exhibited along the horizontal/vertical axis and the diagonal/anti-diagonal axis.

Squeezing of  $\hat{S}_0$ ,  $\hat{S}_1$  and  $\hat{S}_3$  can be achieved by overlapping amplitude squeezed  $\text{TEM}_{10}$  and  $\text{TEM}_{01}$  modes with

phase difference  $\theta = \pi/2$ . The combination of this spatial squeezed beam with a bright  $\text{TEM}_{00}$  beam would simultaneously enable sub-shot noise relative measurements of transverse momentum between the horizontal and vertical axes, as well as left- and right-handed orbital angular momentum of a  $\text{TEM}_{00}$  beam [4].

To achieve quantum enhanced measurements of transverse momentum between the diagonal and anti-diagonal axes, as well as between left- and right-handed orbital angular momentum of a  $\text{TEM}_{00}$  beam, would require squeezing of  $\hat{S}_2$  and  $\hat{S}_3$ . This can be achieved by overlapping quadrature squeezed  $\text{TEM}_{10}$  and  $\text{TEM}_{01}$  modes, at squeezed quadrature angle of  $\pi/4$  (i.e.  $\langle(\delta\hat{X}_{a_{10}}^{\frac{\pi}{4}})^2\rangle < 1$  and  $\langle(\delta\hat{X}_{a_{01}}^{\frac{\pi}{4}})^2\rangle < 1$ ) and  $\theta = \pi/4$ .

Phase squeezed  $\text{TEM}_{10}$  and  $\text{TEM}_{01}$  modes (i.e.  $\langle(\delta\hat{X}_{a_{10}}^-)^2\rangle < 1$  and  $\langle(\delta\hat{X}_{a_{01}}^-)^2\rangle < 1$ ) will yield squeezing of  $\langle(\delta\hat{S}_2)^2\rangle$  only.

#### V. SPATIAL STOKES ENTANGLEMENT

Spatial Stokes entanglement can be generated as shown in Fig. 4. Two squeezed  $\text{TEM}_{10}$  beams, labeled respectively by the subscripts  $x$  and  $y$ , are combined with a  $\pi/2$  relative phase shift on a 50:50 beam-splitter. The beams after the beam-splitter, also in  $\text{TEM}_{10}$  modes, exhibit the usual quadrature entanglement. Two spatial mode combiners, each consisting of a spatial mode separator as shown in Fig. 3 (e) in reverse, are then used to combine the quadrature entangled beams with bright coherent  $\text{TEM}_{01}$  beams, labelled here  $\hat{a}_{01,x}$  and  $\hat{a}_{01,y}$ , respectively. As we will show here, the resulting output beams are entangled in the spatial Stokes operator basis. Experimental verification of the spatial Stokes entanglement can be performed using the detection scheme described in the preceding sections.

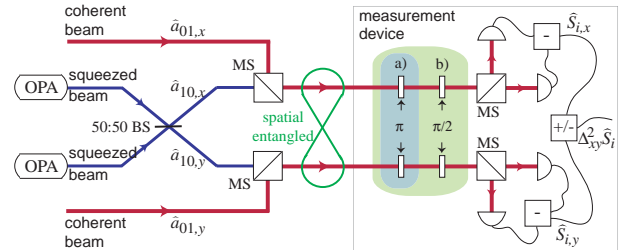


FIG. 4: Scheme to generate and characterize spatial Stokes entanglement. 50:50 BS is a symmetric non-polarizing beam-splitter,  $\pi$  and  $\pi/2$  are modal phase shifters.

To verify the existence of spatial Stokes entanglement we will use the generalized version of the Duan inseparability criterion [32] given in Ref. [33]. This criterion provides a sufficient condition for entanglement and is given by

$$\Delta_{x\pm y}^2 \hat{A} + \Delta_{x\pm y}^2 \hat{B} < 2|[\delta\hat{A}, \delta\hat{B}]| \tag{8}$$

where  $\hat{A}$  and  $\hat{B}$  are two general observables, and  $\Delta_{x\pm y}^2 \hat{O} = \min\langle(\delta\hat{O}_x \pm \delta\hat{O}_y)^2\rangle$ . The degree of inseparability  $\mathcal{I}(\hat{A}, \hat{B})$  is then given by [33]

$$\mathcal{I}(\hat{A}, \hat{B}) = \frac{\Delta_{x\pm y}^2 \hat{A} + \Delta_{x\pm y}^2 \hat{B}}{2|\delta\hat{A}, \delta\hat{B}|}, \quad (9)$$

where  $\mathcal{I}(\hat{A}, \hat{B}) < 1$  indicates an inseparable state.

Assuming for simplicity and symmetry (i.e. both beams  $x$  and  $y$  are identically interchangeable) that  $\alpha_{01,x} = \alpha_{01,y} = \alpha_{01}$  and  $\alpha_{10,x} = \alpha_{10,y} = \alpha_{10}$ , and using Eqs. (4) and (5), we find the inseparability criteria between spatial Stokes operators given by

$$\begin{aligned} \mathcal{I}(\hat{S}_1, \hat{S}_2) &= \frac{\Delta_{x\pm y}^2 \hat{S}_1 + \Delta_{x\pm y}^2 \hat{S}_2}{8|\alpha_{10}\alpha_{01} \sin \theta|} \\ \mathcal{I}(\hat{S}_3, \hat{S}_1) &= \frac{\Delta_{x\pm y}^2 \hat{S}_1 + \Delta_{x\pm y}^2 \hat{S}_3}{8|\alpha_{10}\alpha_{01} \cos \theta|} \\ \mathcal{I}(\hat{S}_2, \hat{S}_3) &= \frac{\Delta_{x\pm y}^2 \hat{S}_2 + \Delta_{x\pm y}^2 \hat{S}_3}{4|\alpha_{10}^2 - \alpha_{01}^2|}. \end{aligned} \quad (10)$$

The correspondence between spatial Stokes and quadrature entanglement becomes obvious when we express the spatial Stokes operator conditional variance  $\Delta_{x\pm y}^2 \hat{S}_i$  in terms of quadrature operators. Making the assumption that  $\alpha_{10} \ll \alpha_{01}$  and using Eq. (6), gives

$$\begin{aligned} \Delta_{x\pm y}^2 \hat{S}_1 &= \alpha_{01}^2 \Delta_{x\pm y}^2 \hat{X}_{a_{01}}^+ \\ \Delta_{x\pm y}^2 \hat{S}_2 &= \alpha_{01}^2 \Delta_{x\pm y}^2 \hat{X}_{a_{10}}^\theta \\ \Delta_{x\pm y}^2 \hat{S}_3 &= \alpha_{01}^2 \Delta_{x\pm y}^2 \hat{X}_{a_{10}}^{\theta - \frac{\pi}{2}}. \end{aligned} \quad (11)$$

Substituting these expressions into Eq. (10), gives

$$\mathcal{I}(\hat{S}_1, \hat{S}_2) = \frac{\alpha_{01}}{8\alpha_{10}|\sin \theta|} \left( \Delta_{x\pm y}^2 \hat{X}_{a_{01}}^+ + \Delta_{x\pm y}^2 \hat{X}_{a_{10}}^\theta \right) \quad (12)$$

$$\mathcal{I}(\hat{S}_3, \hat{S}_1) = \frac{\alpha_{01}}{8\alpha_{10}|\cos \theta|} \left( \Delta_{x\pm y}^2 \hat{X}_{a_{01}}^+ + \Delta_{x\pm y}^2 \hat{X}_{a_{10}}^{\theta - \frac{\pi}{2}} \right) \quad (13)$$

$$\mathcal{I}(\hat{S}_2, \hat{S}_3) = \frac{1}{4} \left( \Delta_{x\pm y}^2 \hat{X}_{a_{10}}^\theta + \Delta_{x\pm y}^2 \hat{X}_{a_{10}}^{\theta - \frac{\pi}{2}} \right). \quad (14)$$

An inspection of Eqs. (12) to (14) show that in the limit considered here only spatial Stokes entanglement between  $\hat{S}_2$  and  $\hat{S}_3$  can be realistically attained. This is because the inseparability criteria of Eqs. (12) and (13) scale with respect to  $\alpha_{01}/\alpha_{10}$ . Since  $\alpha_{01}/\alpha_{10} \gg 1$ , the correlation in  $\hat{X}_{a_{01}}^+$  and  $\hat{X}_{a_{10}}^\theta$  has to be significantly reduced below one, in order to maintain inseparability. On the other hand, we see that after setting  $\theta = 0$ , Eq. (14) reduces to

$$\mathcal{I}(\hat{S}_2, \hat{S}_3) = \frac{1}{4} \left( \Delta_{x\pm y}^2 \hat{X}_{a_{10}}^+ + \Delta_{x\pm y}^2 \hat{X}_{a_{10}}^- \right). \quad (15)$$

So that quadrature entanglement between the TEM<sub>10</sub> modes is transformed directly into spatial Stokes entanglement between the  $\hat{S}_2$  and  $\hat{S}_3$  spatial Stokes operators.

## VI. CONCLUSION

We have identified the relevant spatial modes for optical beam position, momentum and orbital angular momentum. We formalized the quantum properties of these observables using the Stokes-operator formalism and presented a graphical representation of these variables using the Poincaré sphere. A spatial Stokes detection scheme was described and schemes to generate spatial Stokes operator squeezing and entanglement were proposed.

## Acknowledgments

We would like to thank Hans-A. Bachor for fruitful discussions. This work was supported by the Australian Research Council Centre of Excellence Programme.

- 
- [1] N. J. Cerf, and G. Leuchs, *Quantum information with continuous variables of atoms and light* (Imperial College Press, 2007).  
 [2] P. Grangier, R. E. Slusher, B. Yurke, and A. LaPorta, Phys. Rev. Lett. **59**, 2153 (1987); N. V. Korolkova, and A. S. Chirkin, J. Mod. Opt. **43**, 5869 (1996); A. S. Chirkin, A. A. Orlov, and Yu. D. Paraschuk, Kvantovaya Elektron. **20**, 999 (1993); A. P. Alodjants,

- S. M. Arakelian, and A. S. Chirkin, Appl. Phys. B **66**, 53 (1998); N. V. Korolkova *et al.*, Phys. Rev. A **65**, 052306 (2002); W. P. Bowen *et al.*, J. Opt. B. **5**, S467 (2003); W. P. Bowen *et al.*, Phys. Rev. Lett. **88**, 093601 (2002); W. P. Bowen *et al.*, Phys. Rev. Lett. **89**, 253601 (2002); R. Schnabel *et al.*, Phys. Rev. A **67**, 012316 (2003); U. L. Andersen, and P. Buchhave, J. Opt. B **5**, S486 (2003); O. Glockl *et al.*, J. Opt. B. **5**, S492 (2003);

- V. Josse *et al.*, *J. Opt. B* **5**, S513 (2003); N. Korolkova, and R. Loudon, *Phys. Rev. A* **71**, 032343 (2005); J. Laurat *et al.*, *Phys. Rev. A* **73**, 012333 (2006).
- [3] A. Gatti *et al.*, *Phys. Rev. Lett.* **83**, 1763 (1999); A. Gatti, E. Brambilla, and L. A. Lugiato, *Phys. Rev. Lett.* **90**, 133603 (2003); N. Treps *et al.*, *Phys. Rev. Lett.* **88**, 203601 (2002); N. Treps *et al.*, *Science* **301**, 940 (2003); N. Treps *et al.*, *J. Opt. B* **6**, S664 (2004).
- [4] M. T. L. Hsu, V. Delaubert, P. K. Lam and W. P. Bowen, *J. Opt. B* **6**, 495 (2004).
- [5] M. T. L. Hsu, W. P. Bowen, N. Treps, and P. K. Lam, *Phys. Rev. A* **72**, 013802 (2005).
- [6] K. Wagner, J. Janousek, V. Delaubert, H. Zou, C. Harb, N. Treps, J. F. Morizur, P. K. Lam, H. A. Bachor, *Science* **321** 541 (2008).
- [7] J. Hald, J. L. Sorensen, C. Schori, and E. S. Polzik, *Phys. Rev. Lett.* **83**, 1319 (1999); B. Julsgaard, A. Kozhokin, and E. S. Polzik, *Nature* **413**, 400 (2001).
- [8] A. Einstein, B. Podolsky and N. Rosen, *Phys. Rev.* **47**, 777 (1935).
- [9] J. Leach, M. J. Padgett, S. M. Barnett, S. Franke-Arnold, and J. Courtial, *Phys. Rev. Lett.* **88**, 257901 (2002).
- [10] J. Leach, J. Courtial, K. Skeldon, S. M. Barnett, S. Franke-Arnold, and M. J. Padgett, *Phys. Rev. Lett.* **92**, 013601 (2004).
- [11] N. K. Langford, R. B. Dalton, M. D. Harvey, J. L. O'Brien, G. J. Pryde, A. Gilchrist, S. D. Bartlett, and A. G. White, *Phys. Rev. Lett.* **93**, 053601 (2004).
- [12] H. H. Arnaut, and G. A. Barbosa, *Phys. Rev. Lett.* **85**, 286 (2000).
- [13] S. Franke-Arnold, S. M. Barnett, M. J. Padgett, and L. Allen, *Phys. Rev. A* **65**, 033823 (2002).
- [14] A. Mair, A. Vaziri, G. Weihs, and A. Zeilinger, *Nature* **412**, 313 (2001).
- [15] L. Allen, M. W. Beijersbergen, R. J. C. Spreeuw, and J. P. Woerdman, *Phys. Rev. A* **45**, 8185 (1992).
- [16] N. B. Simpson, K. Dholakia, L. Allen, and M. J. Padgett, *Opt. Lett.* **22**, 52 (1997).
- [17] J. Arlt, K. Dholakia, L. Allen, and M. J. Padgett, *Phys. Rev. A* **59**, 3950 (1999).
- [18] S. M. Barnett and R. Zambrini, *J. Mod. Opt.* **53**, 613 (2006).
- [19] J. Leach, M. R. Dennis, J. Courtial, and M. J. Padgett, *Nature* **43**, 165 (2004).
- [20] A. A. Malyutin, *Qu. Elec.* **33**, 235 (2003).
- [21] M. W. Beijersbergen, L. Allen, H. E. L. O. van der Veen, and J. P. Woerdman, *Opt. Comm.* **96**, 123 (1993).
- [22] K. T. Kapale, and J. P. Dowling, *Phys. Rev. Lett.* **95**, 173601 (2005).
- [23] T. Isoshima, M. Nakahara, T. Ohmi, and K. Machida, *Phys. Rev. A* **61**, 063610 (2000).
- [24] D. Akamatsu, and M. Kozuma, *Phys. Rev. A* **67**, 023803 (2003).
- [25] M. E. J. Friese, J. Enger, H. Rubinsztein-Dunlop, and N. R. Heckenberg, *Phys. Rev. A* **54**, 1593 (1996).
- [26] H. He, M. E. J. Friese, N. R. Heckenberg, and H. Rubinsztein-Dunlop, *Phys. Rev. Lett.* **75**, 826 (1995).
- [27] L. Paterson, M. P. MacDonald, J. Arlt, W. Sibbett, P. E. Bryant, and K. Dholakia, *Science* **292**, 912 (2001).
- [28] T. A. Klar, S. Jakobs, M. Dyba, A. Egner, and S. W. Hell, *Proc. of the Nat. Acad. of Sci.* **97**, 8206 (2000).
- [29] M. J. Padgett, and J. Courtial, *Opt. Lett.* **24**, 430 (1999).
- [30] U. Fano, *Phys. Rev.* **93**, 121 (1954).
- [31] V. Delaubert, N. Treps, C. C. Harb, P. K. Lam, and H.-A. Bachor, *Opt. Lett.* **31**, 1537 (2006).
- [32] L.-M. Duan, G. Giedke, J. I. Cirac and P. Zoller, *Phys. Rev. Lett.* **84**, 2722 (2000).
- [33] W. P. Bowen *et al.*, *Phys. Rev. Lett.* **89**, 253601 (2002);